Afyon Kocatepe Üniversitesi Fen ve Mühendislik Bilimleri Dergisi
Afyon Kocatepe University – Journal of Science and Engineering
https://dergipark.org.tr/tr/pub/akufemubid

Araştırma Makalesi / Research Article
e-ISSN: 2149-3367 **DOI: https://doi.org/10.35414/akufemubid.1768844**
CITE: Afyon Kocatepe University Journal of Science and Engineering **26(3)** (2026) 678-692

Effectiveness of Stone Columns in Reducing Liquefaction-Induced Settlements: A Highway Embankment Case Study

Makale Bilgisi / Article Info
Alındı/Received: 19.08.2025
Kabul/Accepted: 24.01.2026
Yayımlandı/Published: 03.06.2026

Sıvılaşma Kaynaklı Oturmaların Azaltılmasında Taş Kolonların Etkinliği: Karayolu Dolgusu Örneği

Yesim TUSKAN*

Manisa Celal Bayar University, Faculty of Engineering and Natural Sciences, Department of Civil Engineering, Manisa, Türkiye

Abstract

The construction of highway embankments often requires measures to improve the load-bearing capacity and control the settlement of the underlying soil. Liquefaction-induced settlement is a potential risk that can compromise the stability and functionality of highways, particularly in seismically active regions. Stone columns are a widely used ground improvement technique to mitigate liquefaction-induced settlements by enhancing the soil's strength and drainage characteristics. This study presents an evaluation of the effectiveness of stone column-supported highway embankments through a detailed case study. Consolidation settlement and liquefaction analyses were performed both for the designed stone column application and for the existing ground conditions. In the embankments and engineering structures along the project alignment, excessive total settlements exceeding tolerable limits are expected in the section between Km: 17+145 and Km: 17+190. The results highlight the significant reduction in liquefaction-induced settlements achieved through the implementation of stone columns.

Keywords: *Highway embankment; Stone column; Liquefaction-induced settlement; Numerical analysis*

Öz

Karayolu dolgu şevlerinin inşası, genellikle altta bulunan zeminin taşıma kapasitesini artırmak ve oturma davranışını iyileştirmek amacıyla zemin iyileştirme önlemleri gerektirir. Özellikle deprem aktivitesinin yüksek olduğu bölgelerde, sıvılaşma kaynaklı yer değiştirmeler, otoyolların stabilitesini ve işlevselliğini tehdit edebilecek potansiyel bir risk oluşturmaktadır. Taş kolonlar, zeminin drenaj özelliklerini ve kesme mukavemetini iyileştirerek, sıvılaşma kaynaklı oturmaları azaltmak için yaygın olarak kullanılan bir zemin iyileştirme tekniğidir. Bu çalışma, taş kolonlarla güçlendirilmiş otoyol dolgularının etkinliğini detaylı bir vaka çalışması aracılığıyla değerlendirmektedir. Tasarlanan taş kolon uygulaması ve mevcut zemin koşulları için konsolidasyon oturması ve sıvılaşma analizleri gerçekleştirilmiştir. Proje güzergâhında yer alan yol dolguları ve sanat yapılarında, Km: 17+145 - 17+190 kesiminde, tolere edilebilir sınırların üzerinde toplam oturmaların meydana gelmesi beklenmektedir. Elde edilen sonuçlar, taş kolon uygulamasının sıvılaşma kaynaklı oturmaları önemli ölçüde azalttığını ortaya koymaktadır.

Anahtar Kelimeler: *Karayolu dolgu şevi; Taş kolon; Sıvılaşma kaynaklı oturma; Nümerik analiz.*

1. Introduction

The bridge approach connects the pavement and subgrades to the abutment, culvert, or other bridge structures, typically via an embankment. However, differential settlement can lead to pavement distress, structural failure, and unsafe driving conditions. Soft soil foundations pose significant challenges to embankment construction due to their high compressibility and low shear strength, which often result in excessive settlement, bearing capacity failure, and both local and global instability. To address these issues, ground improvement methods such as pile inclusions have been widely employed, with numerous studies investigating the load transfer mechanisms and bearing capacities of pile-supported embankments. While most piles are rigid or semi-rigid (e.g., concrete, reinforced concrete, jet-grouted, or deep-mixed columns), stone columns function as granular piles whose vertical load-bearing capacity is primarily governed by the lateral confinement provided by the surrounding soil. In addition to their structural role, stone columns accelerate soil consolidation by providing drainage paths, improving lateral confinement as the surrounding soil consolidates, increasing overall bearing capacity, and reducing ground settlement. Consolidation settlement in saturated soft soils occurs due to the gradual expulsion of pore water under load, often leading to differential or excessive settlement in overlying structures. Given the mechanical characteristics of soft soils, implementing appropriate ground improvement techniques is essential to ensure the long-term stability and safety of infrastructure constructed on such foundations.

*Sorumlu Yazar/Corresponding Author: Yesim Tuskan e-posta/e-mail: yesim.tuskan@cbu.edu.tr

Previous studies have highlighted that soil properties, such as grain size distribution, plasticity, and permeability, play a critical role in determining susceptibility to liquefaction. For instance, Güler et al. (2020) demonstrated that permeability significantly affects the liquefaction potential of silty sands, indicating the importance of both laboratory characterization and in-situ testing for accurate assessment. At the urban scale, the evaluation of liquefaction hazards requires comprehensive technical guidelines and integrated approaches. Lai et al. (2021) provided a framework for assessing earthquake-induced liquefaction in cities, emphasizing the need for detailed geotechnical data, site-specific ground motion parameters, and consideration of heterogeneous soil stratigraphy. Similarly, Okur (2019) applied a GIS-based methodology to analyze soil liquefaction and amplification in Eskişehir, Turkey, highlighting the usefulness of spatial analysis and geospatial data in identifying high-risk zones within urban areas. In the context of disaster resilience, integrating geotechnical assessments with urban risk evaluation frameworks is critical for informed decision-making. Jones et al. (2022) critically evaluated the customization of the UNDRR disaster resilience scorecard for city-level planning, specifically for earthquake-induced liquefaction events. Their study underscores the need to combine engineering-based hazard assessment with resilience-oriented urban planning tools to effectively mitigate the impacts of liquefaction.

Numerous experimental, analytical, and field studies have demonstrated that stone columns enhance both the drainage capacity and the stiffness of the surrounding ground, thereby reducing excess pore-water pressures generated during seismic loading (Adalier and Elgamal, 2004; Baghel and Memon, 2023). This dual mechanism makes stone columns particularly effective in improving seismic and liquefaction performance, which aligns directly with the primary objectives of this research. A comparison with alternative ground-improvement methods further supports this choice. Vibro-compaction is known to perform well in clean, well-graded sands; however, its effectiveness diminishes significantly in soils containing appreciable silt content or in stratified deposits (Hartono and Fathani, 2023). In contrast, stone columns maintain consistent performance in silty sands and heterogeneous soil profiles, where drainage is the critical factor in mitigating liquefaction. Their high permeability allows for efficient dissipation of earthquake-induced pore pressures, a mechanism emphasized in recent liquefaction triggering and mitigation frameworks (Selçuk and Kayabali, 2015). Other techniques, such as deep soil mixing, were also evaluated; however, deep mixing is generally associated with higher construction costs, slower production rates, and potential environmental impacts stemming from binder injection (Deb et al., 2020). Gravel drains provide effective drainage but contribute minimally to stiffness improvement, limiting their capacity to enhance the cyclic resistance of the soil. Recent studies show that stone columns outperform gravel drains by providing simultaneous drainage and stiffness enhancement, resulting in improved seismic response (Deb et al., 2020). Consequently, stone columns were deemed the most appropriate ground-improvement method for the soil conditions and performance requirements considered in this study.

Numerical analysis methods have been widely used in previous studies to investigate various civil engineering problems, including slope stability, soil–pile interaction, deep excavations, buried pipeline, wind turbine foundations, and pile-supported embankments under different settlement conditions (Tuskan and Basari 2023; Liu et al. 2007; Tuskan and Yiğit 2025; Tuskan 2025; Girout et al. 2018; Dagli et al. 2018; Hanna and Khalifa 2023). Over the past few decades, numerical methods have gained increasing importance in geotechnical engineering practice and have become indispensable tools in civil engineering design, widely recognized and accepted within the field. In this study, both experimental and numerical approaches are employed to evaluate the effectiveness of stone columns in reinforcing highway embankments and bridge approach sections.

2. Site Condition

The study area is located above the İzmir–Ankara suture zone and is bordered by various lithological units: rock masses to the north, the Menderes Massif to the east-southeast, and the Karaburun Belt to the west-southwest The Gediz Graben lies to the south-southeast, while the Bergama region bounds the north. The project corridor traverses the Gediz Valley, where bedrock comprises alluvial sediments, underlain by claystone–siltstone conglomerates from the base of the alluvium interpreted as bedrock. These alluvial sediments are categorized into fine-grained (Qal1) and coarse-grained (Qal2) units, further subdivided based on their physical and geomechanical properties, determined through surface mapping, borehole drilling, in-situ, and laboratory testing. Beneath these, altered conglomerate layers belonging to the Çukurköy Volcanics (T_{mcd}) form the valley floor. The embankment sections are founded on these alluvial deposits, which overlie shaley siltstone bedrock; they consist of medium to hard—occasionally soft—low- to medium-plasticity silty clay, clayey silt, gravelly clayey sand, gravelly sand, and sandy gravel. Along the corridor from Km 16+800 to Km 18+907, the highway is planned as a combination of bridge and elevated embankment sections, reaching a maximum embankment height of approximately 14 m. The Quaternary evolution of the Gediz Graben basin, shaped by syn-sedimentary tectonics under N–S extensional regime, influenced sediment facies and depositional patterns (Hakyemez et al. 2013), while its episodic two-stage extensional history, marked by Miocene–Early Pliocene and Plio-Quaternary phases separated by short compressional intervals, has been well-documented (Koçyiğit et al. 1999). As part of the conducted studies, the parameters of the units at the base were selected and the soil profile was idealized to determine the amount of consolidation settlement that the embankments would cause in the clay unit at the base (Figure 1,2).

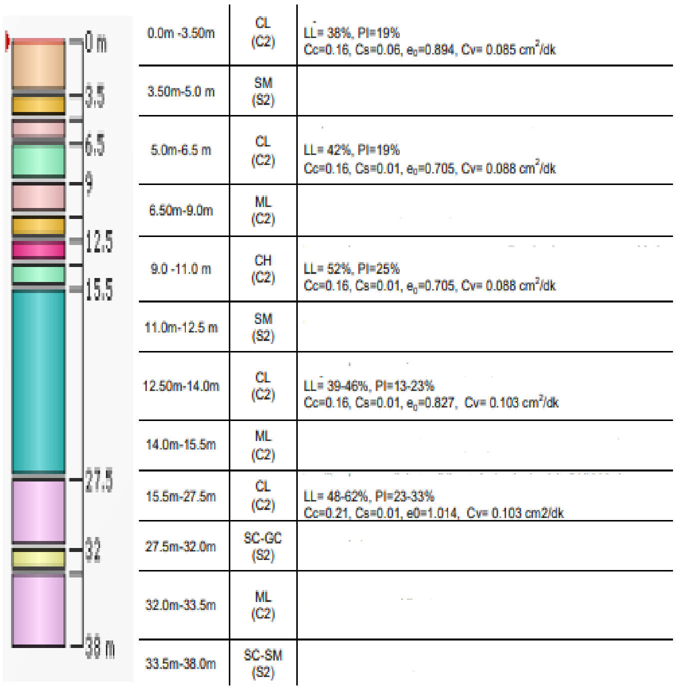

Figure 1. Idealized soil profile at km: 17+145

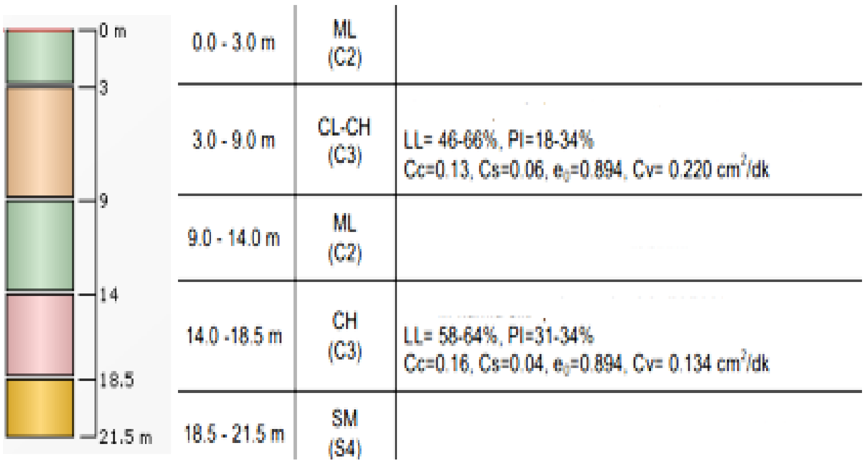

Figure 2. Idealized soil profile at km: 16+980

3. Materials and Methods

Stone columns have become a popular solution for strengthening weak soil and minimizing settlement in structures (Singh and Mishra 2023; Taube and Herridge 20022). They serve as a method of soil stabilization by increasing soil strength, reducing compressibility of loose fine graded soils, expediting consolidation effects, and decreasing the possibility of soil liquefaction. There are two commonly used methods for constructing stone columns: replacement and displacement. In the displacement method, also known as the dry method, a vibratory probe is used to laterally displace the native soil with the help of compressed air. This installation technique is suitable for areas with low groundwater levels and firm in situ soil. Nowadays, it is possible to solve complicated geotechnical problems due to the rapid development of computer software. Settlement calculation is a crucial process in geotechnical engineering that helps determine the expected displacement or settlement of the ground due to various factors such as construction activities, soil composition, and groundwater levels. Accurate settlement calculations are vital for designing stable structures and ensuring the safety and longevity of civil engineering projects. Traditionally, settlement calculations were performed using analytical methods based on simplified assumptions and empirical equations. However, these methods often fail to capture the complexity and diversity of real-world soil behavior. To overcome these limitations, numerical analysis techniques have become increasingly popular and reliable.

Numerical analysis, also known as numerical modeling, involves dividing the soil into discrete elements and solving complex mathematical equations using computer algorithms. This approach considers the soil as a continuum and provides a more realistic representation of its behavior. Settlement calculation using numerical analysis has revolutionized the field of geotechnical engineering. This approach offers a more comprehensive understanding of soil behavior and enables accurate predictions of settlement patterns. It assists engineers in designing safe and stable structures, optimizing construction processes, and mitigating potential risks associated with ground settlement. Settle 3D software (Blöcher and Zimmermann 2008) is used for consolidation analysis based on one-dimensional equations with either a linear or non-linear technique. Settle 3D's linear consolidation model is one of the conventional solutions for consolidation. The solution for the consolidation in Settle 3D is as follows:

$$\Delta\varepsilon = \frac{C_r}{1+e_0} log\left(\frac{P_c}{\sigma_i'}\right) + \frac{C_c}{1+e_0} log\left(\frac{\sigma_f'}{\sigma_i'}\right) \tag{1}$$

The Recompression ratio is determined by $\frac{C_r}{1+e_0}$ and the compression ratio is represented by $\frac{C_c}{1+e_0}$. Settle 3D employs the analytical technique, which is based on the secondary compression index parameter C_α. The following equation is used to compute the change in vertical strain from time t_1 to t_2 during the secondary compression (Equation 2):

$$\Delta\varepsilon_s = \frac{C_\alpha}{1+e_p} log\left(\frac{t_2}{t_1}\right) \tag{2}$$

where e_p is the void ratio at the end of primary consolidation. When secondary compression occurred, the linear soil model provided acceptable ultimate settlement results. However, analytical solutions using a linear model produced lesser final settlement values as compared to finite element analysis. Furthermore, it has been observed that the primary consolidation was completed in a very short amount of time. Compared to both the nonlinear model of the analytical approach and the FE studies, the nonlinear soil model produced results for final settlement values that were closer to the in-situ measurement. Thus, nonlinear analysis was performed in this study.

The cyclic stress ratio and related parameters were calculated using the following equations: the depth-dependent reduction factor (r_d) was determined from Equation (3), where α(z) and β(z) are depth-dependent functions given by Equations (4) and (5), respectively. The magnitude scaling factor (MSF) was computed according to Equation (6), while the normalized standard penetration test value and was obtained using the standard correction factors as expressed in Equation (7) and further adjusted for fines content according to Equation (8).

$$r_d = \exp\left[\alpha(z) + \beta(z) \cdot M_w\right] \tag{3}$$

$$\alpha(z) = -1.012 - 1.126 \sin(z/11.73 + 5.133) \tag{4}$$

$$\beta(z) = 0.106 + 0.118 \sin(z/11.28 + 5.142) \tag{5}$$

$$MSF=10^{(Mw/2.24)-2.56} \tag{6}$$

$$(N_1)_{60} = C_N \cdot C_E \cdot C_B \cdot C_R \cdot C_S \cdot N_{30} \tag{7}$$

$$(N_1)_{60,cs} = (N_1)_{60} + \Delta(N_1)_{60} \tag{8}$$

The clean-sand corrected normalized standard penetration test value, $(N_1)_{60,cs}$, was calculated based on the fines content (FC) of the soil using the following criteria: for soils with **FC ≤ 5%**, no correction was applied, so $(N_1)_{60,cs} = (N_1)_{60}$; for soils with **5% < FC < 35%**, an incremental correction was applied according to $\Delta(N_1)_{60} = \exp\left[1.76 - \frac{190}{FC^2}\right]$; and for soils with **FC ≥ 35%**, a standard correction of 5 blows was added, giving $(N_1)_{60,cs} = (N_1)_{60} + 5$(Youd et al., 2001).

Additionally, Factor of Safety (FS) against liquefaction is determined by using Cyclic Stress Ratio (CSR) and Cyclic Resistance Ratio (CRR):

$$\mathrm{FS} = \frac{\mathrm{CRR}}{CSR} x\ MSF \tag{9}$$

$$\mathrm{CSR} = 0.65 \frac{\sigma_v}{\sigma_v'} x\ \frac{a_{max}}{g} r_d \tag{10}$$

$$\mathrm{CSR} = \frac{1}{34-N_{1,60cs}} + \frac{N_{1,60cs}}{135} + \frac{50}{\left[10N_{1,60cs}+45\right]^2} - \frac{1}{200} \quad (11)$$

where MSF is the Magnitude Scaling Factor, r_d is stress reduction factor, g is the acceleration of gravity, $N_{1,60cs}$ is the normalization of penetration resistance through fines content, a_{max} is the peak horizontal ground acceleration. Moreover, soft soil parameters were shown in Table 1 and 2.

Table 1. Soft soil parameters at km: 16+980

Depth (m)	Soil	(Cc, Cr, e_0, κ, ν, OCR)	k_h (m/s)	k_v (m/s)	Drainage	r_d	MSF (M_w=7.1)
0–3 m	ML	Cc:0.10, Cr:0.03, e0=0.80, κ=0.010, ν=0.25, OCR=1	1×10^{-6}	3×10^{-7}	Undrained	0.95	0.57
3–9 m	CL–CH	Cc=0.13, Cr=0.06, e0=0.894, κ=0.013, ν=0.25, OCR=1	5×10^{-8}	2×10^{-8}	Undrained	0.90	0.57
9–14 m	ML	Cc:0.12, Cr:0.04, e0=0.85, κ=0.012, ν=0.25, OCR=1	8×10^{-7}	2.5×10^{-7}	Undrained	0.82	0.57
14–18.5 m	CH	Cc=0.16, Cr=0.04, e0=0.894, κ=0.016, ν=0.25, OCR=1	3×10^{-8}	1×10^{-8}	Undrained	0.75	0.57
18.5–21.5 m	SM	e0=0.60, κ=0.003, ν=0.30,	1×10^{-4}	5×10^{-5}	Drained	0.68	0.57

Table 2. Soft soil parameters at km: 17+145

Depth (m)	Soil	(Cc, Cr, e_0, κ, ν, OCR)	k_h (m/s)	k_v (m/s)	Drainage	r_d	MSF (M_w=7.1)
0–3.5	CL	Cc=0.16, Cr=0.06, e_0=0.894, κ=0.016, ν=0.25, OCR=1	4×10^{-8}	2×10^{-8}	Undrained	0.95	0.57
3.5–5.0	SM	e_0=0.55, κ=0.005, ν=0.30	1×10^{-5}	5×10^{-6}	Drained	0.90	0.57
5.0–6.5	CL	Cc=0.16, Cr=0.01, e_0=0.705, κ=0.016, ν=0.25, OCR=1	4×10^{-8}	2×10^{-8}	Undrained	0.88	0.57
6.5–9.0	ML	Cc=0.12, Cr=0.04, e_0=0.78, κ=0.012, ν=0.25, OCR=1	1×10^{-6}	3×10^{-7}	Undrained	0.86	0.57
9.0–11.0	CH	Cc=0.16, Cr=0.01, e_0=0.705, κ=0.016, ν=0.25, OCR=1	3×10^{-8}	1×10^{-8}	Undrained	0.83	0.57
11.0–12.5	SM	e_0=0.55, κ=0.005, ν=0.30	1×10^{-5}	5×10^{-6}	Drained	0.82	0.57
12.5–14.0	CL	Cc=0.16, Cr=0.01, e_0=0.827, κ=0.016, ν=0.25, OCR=1	4×10^{-8}	2×10^{-8}	Undrained	0.81	0.57
14.0–15.5	ML	Cc=0.12, Cr=0.04, e_0=0.75, κ=0.012, ν=0.25, OCR=1	1×10^{-6}	3×10^{7}	Undrained	0.79	0.57
15.5–27.5	CL	Cc=0.21, Cr=0.01, e_0=1.014, κ=0.021, ν=0.25, OCR=1	3×10^{-8}	1.5×10^{-8}	Undrained	0.77	0.57
27.5–32.0	SC–GC	e_0=0.55, κ=0.005, ν=0.30	5×10^{-5}	2×10^{-5}	Drained	0.59	0.57
32.0–33.5	ML	Cc=0.10, Cr=0.03, e_0=0.70, κ=0.010, ν=0.25, OCR=1	1×10^{-6}	3×10^{-7}	Undrained	0.52	0.57
33.5–38.0	SC–SM	e_0=0.55, κ=0.005, ν=0.30	5×10^{5}*	2×10^{5}*	Drained	0.50	0.57
38.0–45.0	Andesite		—	—	Undrained	0.43	0.57

4. Results and Discussions

4.1 Consolidation Analysis

Consolidation calculations were performed using the Settle 3D software (Blöcher and Zimmermann 2008) for selected sections based on the idealized soil profile and parameters. The elastic settlements will be completed during the fill construction. In this study, consolidation settlements that will occur over time in terms of clay units have been investigated. In the analysis, settlement criteria of 5.0 cm allowable settlement amount, as specified in the specifications for bridge approach fills, and 10.0 cm allowable settlement amounts were used as the limit values for other sections (Karayolları Teknik Şartnamesi 2006). Liquefiable soil has a complex structure with non-homogeneous and nonlinear characteristics (Yu and Mitchell 1998). Its complex soil behavior was represented by a multitude of constitutive soil models (Dafalias and Manzari 2004). However, the widely used soft soil model was used in this study to demonstrate stress-strain behavior (Blöcher and Zimmermann 2008).

At Km: 16+980, the height of the road embankment is H=9.0 meters. In this section, which is modeled as the approaching embankment of the main irrigation canal, clay levels have been determined between 3.50 - 9.0 m and 14.0 - 18.50 meters at the embankment base (Figure 3).

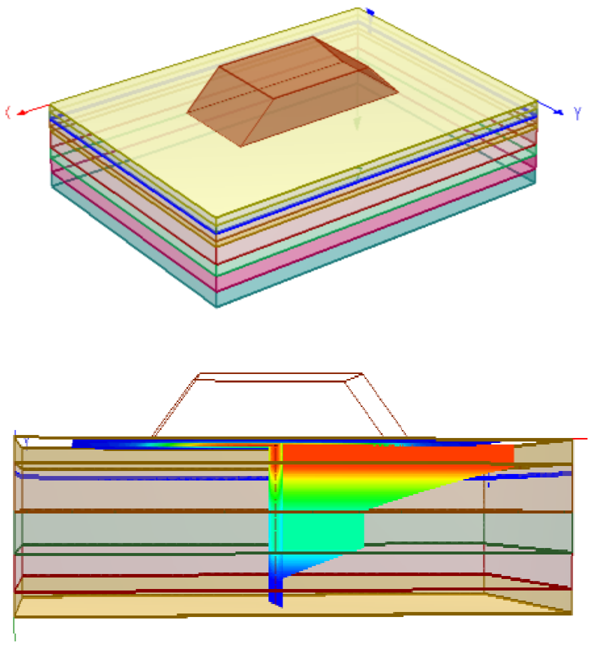

Figure 3. Embankment numerical model and soil profile at km: 16+980

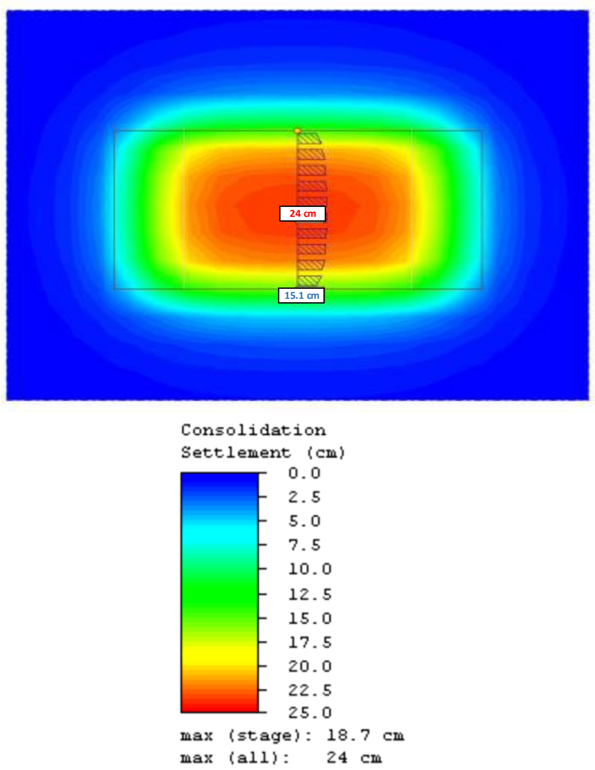

Figure 4. Consolidation settlement at km: 16+980

However, in order to accelerate the settlement time, if the overlay thickness is made 3.0 meters in this section and controlled rock fill is used instead, the expected consolidation settlement value in clay units is calculated as 24.0 cm (Figure 4.).

In the case where the allowable settlement is 5.0 cm, it will take approximately 9-10 months to complete the settlement of 19.0 cm. Moreover, it will take approximately 48 months to complete the settlement of 55.1 cm. In this context, it is recommended to construct stone columns with a size of D=50 cm in diameter, with a grid pattern of $a_v x a_h$=1.1 x 1.1 m, and a length of L=16.0 meters to minimize consolidation settlements (Figure 5).

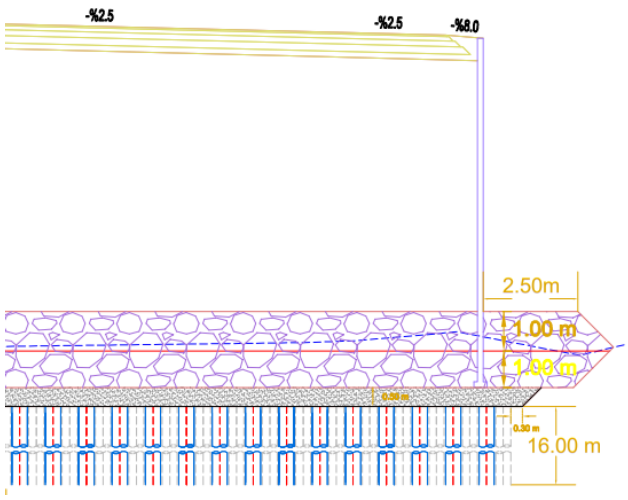

Figure 5. Stone column design of embankment at km: 16.980-17+145

Thus, the carrying capacity/deformation modulus of the entire improved soil mass will be increased, resulting in a reduction in total settlement. Additionally, stone columns will serve as drains, ensuring that consolidation settlements in the soil after the formation of the embankment are completed within a short period of time after construction. In order to accelerate the settlement of the ground and to increase the relative density of the foundation soils depending on the application and to reduce the pore water pressure that will occur in the dynamic situation in the liquefied levels, stone column application was evaluated with different application patterns (Priebe 1997; Baziar and Alizadeh 2015). As a result, stability was achieved in case of stone column application with 1.10x1.10 pattern (triangle model) designing maximum stability with minimum cost.

Subsequently, at Km: 17+145, the height of the road embankment is H=9.0 meters. In this section, which is modeled as the approaching embankment of the main irrigation canal bridge, clay levels have been determined between 5.0 - 6.50 m, 9.0 - 11.0 m, and 12.50 - 27.50 meters at the embankment base. The expected total consolidation settlement amount at these levels is calculated as 60.1 cm (Figure 6).

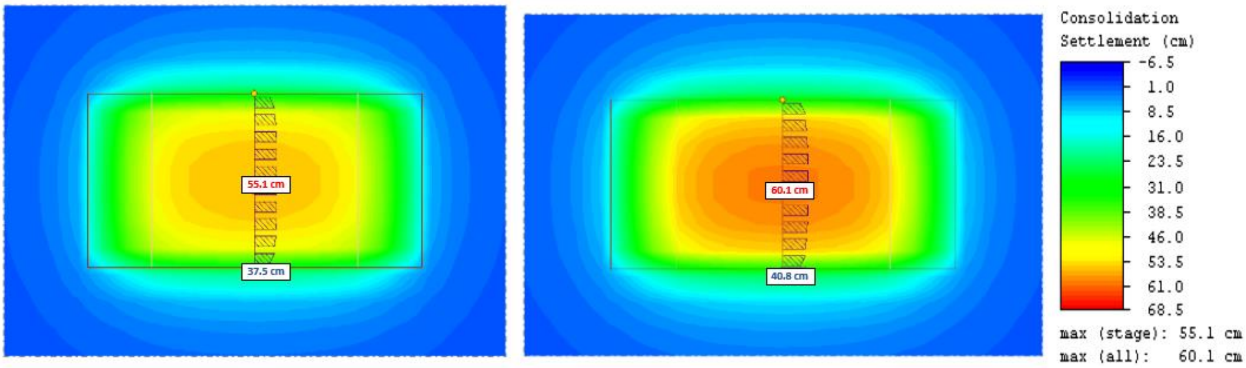

Figure 6. Consolidation settlement at Km: 17+145

The amount of settlement after the stone column application has been predicted using the Van Impe and De Beer (1983) approach (Figure 7).

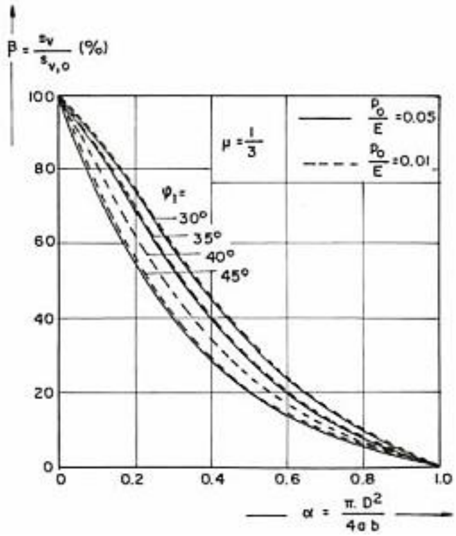

Figure 7. Stress distribution of stone columns (Van Impe and De Beer 1983)

According to this approach, for stone columns with a diameter of 50 cm and a grid size of 1.1x1.1 m, a β value of 0.25 (Equation 12) was taken and the settlement after improvement was found to be 15 cm. The following characteristics are specified to indicate the improvement in the settlement behavior of the soft soil reinforced with stone columns:

$$\beta = \frac{S_v}{S_{v,0}} \tag{12}$$

Where, S_v = the vertical settlement of the composite layer of soft cohesive soil and stone columns, $S_{v,0}$ = the vertical settlement of the natural soft layer without stone columns.

It is expected that these settlements will be completed within 5-6 months. In order to determine the performance of the stone column, individual columns were constructed in the field and loading tests were conducted to determine their bearing capacity and rigidity. Similar calculations continued along the section and are given below. The height of the embankment at Km 17+190 is H=8.20 meters. In this section, where the outlet of the main irrigation canal is considered as the approach fill, clay levels were determined between 7.80 - 11.80 m, 16.20 - 19.20 m, and 23.50 - 32.0 meters on the embankment base. The total consolidation settlement expected to occur at this level was calculated as 20.1 cm. In the case where the permissible settlement is 5.0 cm, it takes approximately 7-8 months to complete a settlement of 15.1 cm, while with an acceptance of 10.0 cm, this time is less than 2 months. The height of the embankment at Km 18+680 is H=6.0 meters. This section was considered as the critical fill section and was modeled. In this section, clay levels were determined between 20.0 - 25.0 meters on the embankment base. The total consolidation settlement expected to occur at this level was calculated as 12.8 cm. In the case where the permissible settlement is 5.0 cm, it takes approximately 3-4 months to complete a settlement of 7.8 cm, while with an acceptance of 10.0 cm, this time is less than 1 month. In section Km: 18+907, the height of the road fill is H=14.0 meters. It has been evaluated and modeled as the approach fill section for the Belen Viaduct. In this section, fill base levels have been determined between 8.0 - 9.50, 12.5 - 14.5, and 21.5 - 24.5 meters. It can be observed that the most critical section in terms of secondary settlements is at KM: 16+980 considering the consolidation settlements. After a 3.0 m displacement fill is made on the surface in this section, considering the typical values in the fill area of the project, considering the thickness of sand/gravel layer at around 35% of the settled layer thickness, the secondary settlements that will occur in a period of t = 10 years after primary consolidation settlements are expected to be at the level of 3.8 cm. These settlements are not considered critical. In order to evaluate the characteristics of the stone column in the field and apply it to the model, allowable settlements were considered. In the case where the allowable settlement is 5.0 cm, the time required to complete 55.1 cm settlement at Km: 17+145 is approximately 48 months (Figure 8).

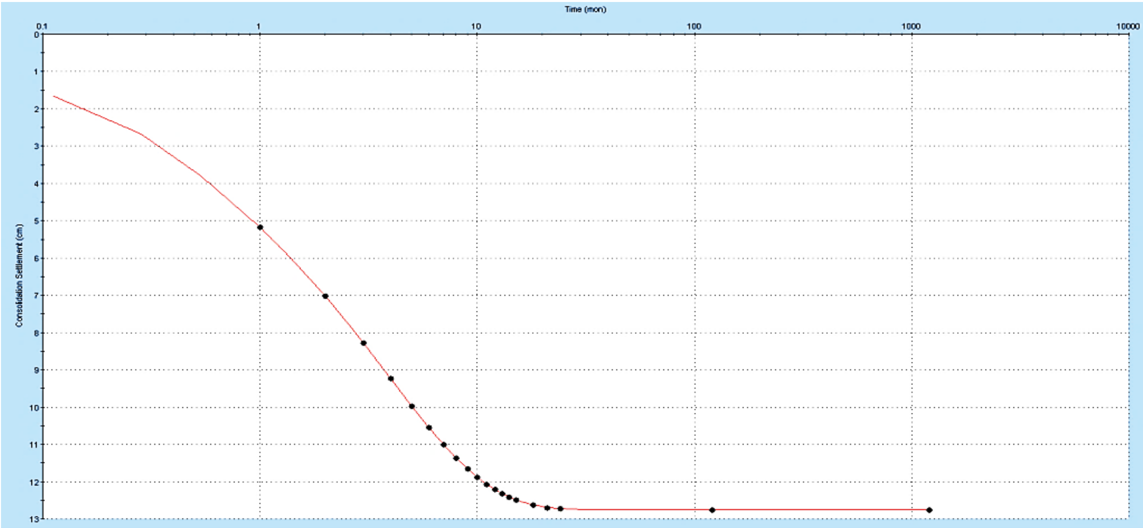

Figure 8. Settlement-time graph of embankment at km: 17+145

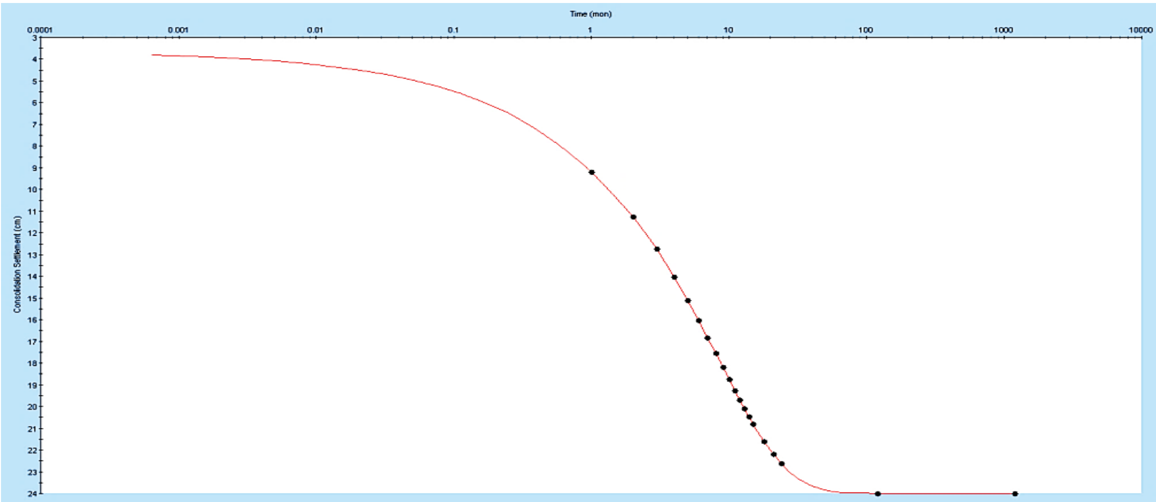

Figure 9. Settlement-time graph of embankment at km: 16+980

In this context, in order to minimize and end consolidation settlements, it is recommended to manufacture a 50 cm diameter 1.1 x 1.1 m spacing and 16.0 meter long stone column. Thus, the bearing capacity/deformation modulus of the entire improved soil mass will be increased and the total settlement to be formed will be reduced. Similarly, in the case where the allowable settlement is 5.0 cm in Km: 16+980, the time required to complete 22.7 cm settlement is approximately 12 months (Figure 9) The diameter, spacing, placement type and column lengths of the stone column were selected as a result of the above evaluations.

4.2 Liquefaction Analysis

The estimation and assessment of liquefaction is an essential component of the earthquake-resistant modeling of structures on liquefiable soils (Youd and Idriss 1997; Seed and Idriss 1971; Stewart 2015). The detrimental impacts of liquefaction on highway embankments can be listed as settlement, slope failure, and damage to infrastructure (Tokimatsu and Yoshimi 1990; Bray and Macedo 2012; Cubrinovski and Ishihara 2000). In the section Km: 18+600 - 18+907, the fine-grained levels that are predominantly present in the alluvial deposits are replaced by more coarse-grained levels in the direction from the "Main Canal Bridge" to the "Belen Bridge" (Figure 10).

Therefore, at the beginning of this region called Gediz River crossing, geotechnical problems related to consolidation settlements primarily arise due to the density and nature of the fine-grained levels named Qal1 in the model. As we move towards the Belen Viaduct, the behavior of the soil under dynamic conditions becomes a problem due to the density of the coarse-grained levels named Qal2. The approach fills of the Belen Viaduct reach a height of 14.0 meters, and the ground water level in this section has been measured and recorded periodically between 3.90 - 9.00 meters in various stages of the project's investigation boreholes. The measured 3.90-meter level in the investigation borehole SK-18+907 carried out during the implementation phase was considered the most critical condition.

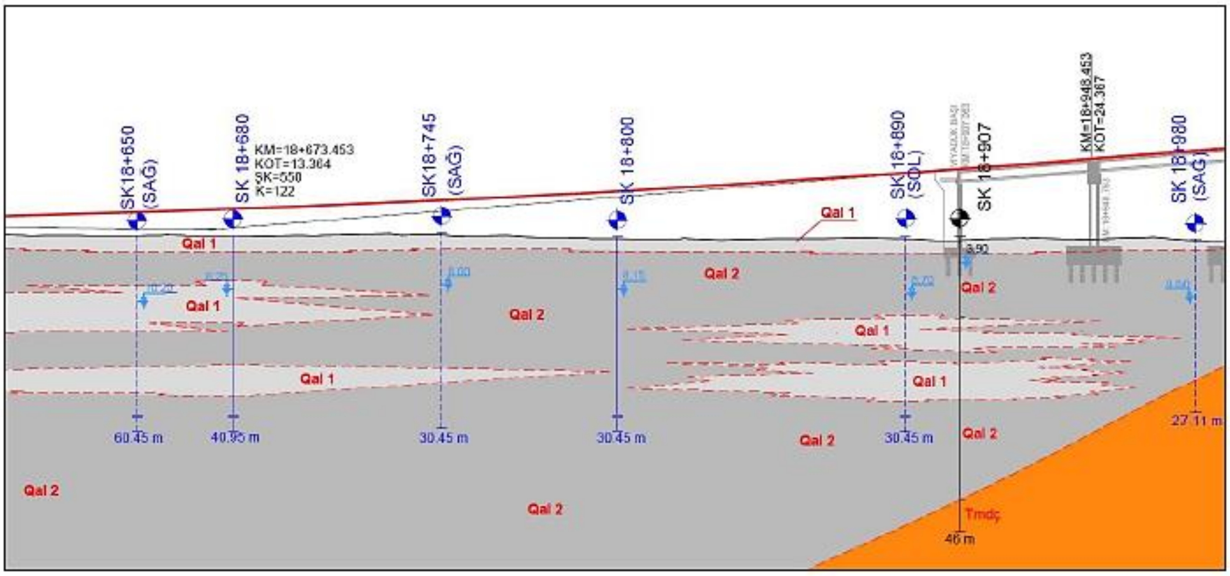

Figure 10. Soil profile at bridge approach between Belen bridge and main canal bridge

In the research studies, the limit values derived from laboratory tests conducted on disturbed samples obtained from the levels where SPT tests were performed, as well as on undisturbed (UD) samples taken from the fine-grained layers, are presented below: The fine-grained soil layers (Qal1) exhibit a wide range of geotechnical properties based on the laboratory and in-situ test results. Standard Penetration Test (SPT) blow counts vary significantly between N = 4 and N = 48, indicating considerable variability in soil stiffness across the strata. The natural water content shows a broad distribution as well, ranging from 2.73% to 43.62%. Atterberg limit tests also reflect substantial differences in plasticity characteristics: the liquid limit (LL) varies from non-plastic (NP) to 81%, while the plasticity index (PI) ranges from NP to 54. Grain-size distribution analyses reveal that the portion retained on the No. 4 sieve falls between 0% and 22%, whereas the fraction passing the No. 200 sieve ranges from 51% to 99.5%, confirming the predominantly fine-grained nature of these layers. The natural unit weight is measured between 18.0 and 19.40 kN/m³. Unconfined compressive strength values indicate a cohesion range of approximately 23 to 112 kPa. Based on the Unified Soil Classification System (USCS), these soils are classified as CL, CH, MH, and ML, reflecting their clayey and silty characteristics with varying plasticity. The coarse-grained units (Qal2) present different geotechnical behavior compared to the fine-grained layers. SPT blow counts range from N = 8 to refusal, indicating generally denser and more compact material. The natural water content varies between 2.94% and 37.41%, while the liquid limit (LL) values extend from NP to 48%, with corresponding plasticity index (PI) values between NP and 31, suggesting that these soils exhibit low to moderate plasticity when fines are present. Grain-size analysis reveals that 0% to 70% of the material is retained on the No. 4 sieve, and 21% to 49% passes the No. 200 sieve, confirming the presence of sandy or gravelly soils with varying fine content. According to the USCS, these layers are classified as SM, SC, SP–SM, SW–SM, GC, and GM, representing mixtures of sands and gravels containing silty or clayey fractions.

The normalized standard penetration test values, $(N_1)_{60}$, were obtained using standard correction factors, and the clean-sand corrected values, $(N_1)_{60,cs}$, were adjusted based on the fines content of the soil following the criteria of Youd et al. (2001). These calculations are summarized in tables 3and 4.

Liquefaction analysis has been carried out according to the liquefaction criteria determined in the NCEER (Youd and Idriss 1997) earthquake workshop, using the field and laboratory test results obtained from the SK-18+907 drill to evaluate the approach fills of the Belen Viaduct reaching a height of 14.0 meters. Probabilistic seismic hazard maps in Turkey (Erdik et al., 2006) provide peak ground acceleration (PGA, T = 0) contours for different return periods. The 72-year return period contour (~50% exceedance probability in 50 years) represents a “frequent” earthquake scenario, reflecting moderate-to-strong ground motions expected at a site. Using this contour as a basis for site-specific analyses or liquefaction studies is methodologically justified, but it does not account for rare, more severe events, which should be acknowledged as a limitation. The analysis was conducted considering design acceleration PGA=0.426g and earthquake magnitude Mw=7.1, as determined by the seismic study conducted in the investigation area.

Table 3. SPT Correction at km: 16 + 980

Borehole: 16+980 Ground Water Level: 4.20 m									
Depth	N_{30}	Effective Vertical Stress σ'_{0v} (kPa)	Overburden Correction Factor C_N	Energy Correction Factor C_E	Borehole Correction Factor C_B	Rod Length Correction Factor C_R	Sampler Correction Factor C_S	$N_{1,60}$	$(N_{1,60})_{cs}$
1.5	8	26.25	1.70	0.75	1.0	0.75	1.0	8	13
3	6	52.5	1.38	0.75	1.0	0.80	1.0	5	10
4.5	6	76.26	1.15	0.75	1.0	0.85	1.0	4	9
6	33	90.04	1.05	0.75	1.0	0.95	1.0	25	30
7.5	24	103.83	0.98	0.75	1.0	0.95	1.0	17	22
9	13	117.61	0.92	0.75	1.0	0.95	1.0	9	14
10.5	17	131.40	0.87	0.75	1.0	1.0	1.0	11	16
12	9	145.18	0.83	0.75	1.0	1.0	1.0	6	11
13.5	9	158.97	0.79	0.75	1.0	1.0	1.0	5	10
15	20	172.75	0.76	0.75	1.0	1.0	1.0	11	16
16.5	31	186.54	0.73	0.75	1.0	1.0	1.0	17	22
18	38	200.32	0.71	0.75	1.0	1.0	1.0	20	25
19.5	52	214.11	0.68	0.75	1.0	1.0	1.0	27	32
21	89	227.89	0.66	0.75	1.0	1.0	1.0	44	44

Table 4. SPT Correction at km: 17 + 145

Borehole: 17+145 Ground Water Level: 4.90 m									
Depth	N_{30}	Effective Vertical Stress σ'_{0v} (kPa)	Overburden Correction Factor C_N	Energy Correction Factor C_E	Borehole Correction Factor C_B	Rod Length Correction Factor C_R	Sampler Correction Factor C_S	$N_{1,60}$	$(N_{1,60})_{cs}$
1.5	4	26.25	1.70	0.75	1.0	0.75	1.0	4	9
3	4	52.50	1.38	0.75	1.0	0.80	1.0	3	3
4.5	10	78.75	1.13	0.75	1.0	0.85	1.0	7	11
6	3	106.65	0.97	0.75	1.0	0.95	1.0	7	11
7.5	7	135.15	0.86	0.75	1.0	0.95	1.0	2	6
9	4	123.45	0.90	0.75	1.0	0.95	1.0	4	4
10.5	6	137.21	0.85	0.75	1.0	1.0	1.0	3	8
12	7	154.97	0.80	0.75	1.0	1.0	1.0	4	9
13.5	13	164.78	0.78	0.75	1.0	1.0	1.0	4	9
15	10	178.57	0.75	0.75	1.0	1.0	1.0	8	8
16.5	11	192.35	0.72	0.75	1.0	1.0	1.0	6	11
18	10	206.14	0.70	0.75	1.0	1.0	1.0	5	10
19.5	9	219.92	0.67	0.75	1.0	1.0	1.0	5	10
21	7	223.71	0.65	0.75	1.0	1.0	1.0	3	8
22.5	9	393.75	0.50	0.75	1.0	1.0	1.0	3	8
24	11	423.50	0.49	0.75	1.0	1.0	1.0	4	9
25.5	12	275.06	0.60	0.75	1.0	1.0	1.0	5	10
27	14	288.85	0.59	0.75	1.0	1.0	1.0	6	11
28.5	27	302.63	0.57	0.75	1.0	1.0	1.0	12	17
30	25	316.42	0.56	0.75	1.0	1.0	1.0	11	16
31.5	24	330.20	0.55	0.75	1.0	1.0	1.0	10	15
33	21	343.99	0.54	0.75	1.0	1.0	1.0	8	13
34.5	33	357.77	0.53	0.75	1.0	1.0	1.0	13	18
36	36	371.56	0.52	0.75	1.0	1.0	1.0	14	14
37.5	>50	385.24	0.51	0.75	1.0	1.0	1.0	>50	-

In the analysis, the liquefaction resistance ratio (CRR) of the soil obtained by dividing the corrected SPT-N blow counts (N1,60) by the cyclic stress ratio (CSR) was obtained (Seed et al. 1983) The CRR was corrected according to the fines content of the soil due to the presence of non-plastic fines in the soil (Youd and Hoose 1993; Ishihara 1996). The liquefaction analysis is shown in Figure 11.

As a result of the analysis, the liquefaction levels are presented in Figure 11, and the expected settlement amount after liquefaction is calculated to be 30.99 cm. In this context, in order to minimize the damage (settlement, collapse) caused by an earthquake and to make it usable in emergency situations, there is a need for improvement at the foundation level. As a result, in the case of a 1.10x1.10 pattern (triangular model) with a 20.0-meter stone column application, the analysis results are shown in Figure 12.

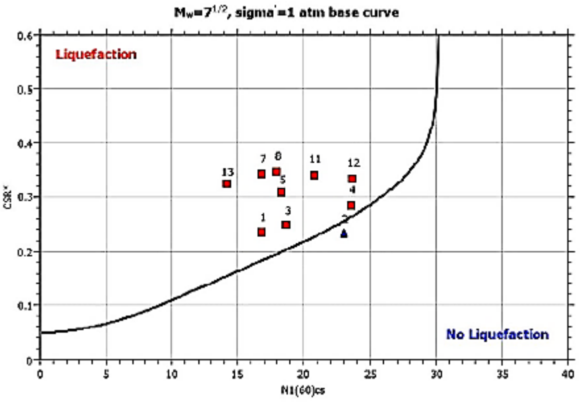

Figure 11. The liquefaction analysis at bridge approach

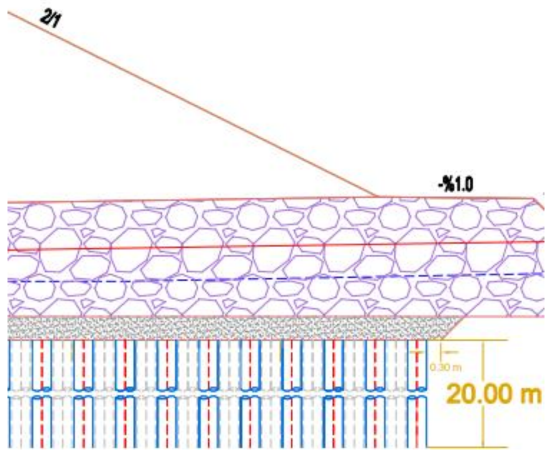

Figure 12. Stone column application at bridge approach of Km: 18+907

Therefore, stone column application (Figure 13) with different implementation patterns has been evaluated in order to accelerate settlements in the soil and increase the relative density of the foundation soils, aiming to reduce the excess pore water pressure that would occur in a dynamic situation at the liquefied levels.

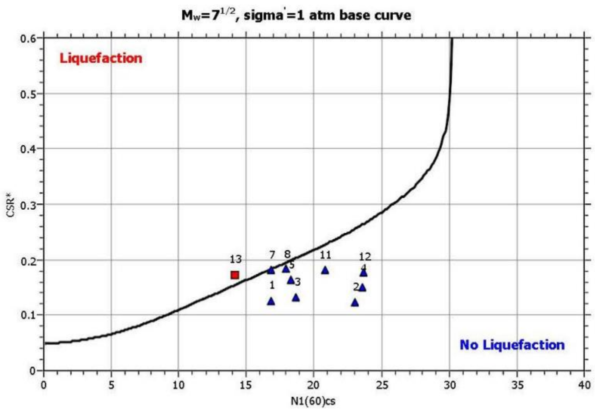

Figure 13. The liquefaction analysis at bridge approach with stone column application

Figure 14. shows the difference in settlement before and after the stone column installation, respectively.

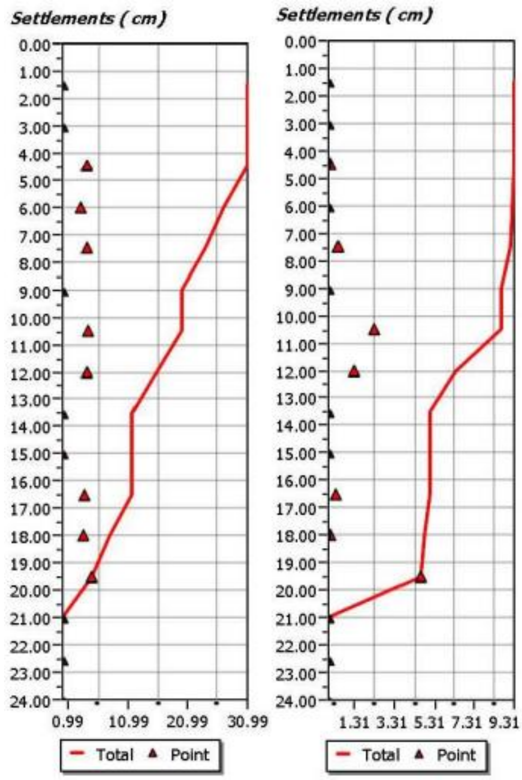

Figure 14. Settlement before and after Stone column application

Therefore, at the beginning of the region known as the Gediz River crossing, geotechnical problems associated with consolidation settlements primarily arise due to the density and nature of the fine-grained layers identified as Qal1 in the model. In fact, the high compressibility and low permeability of these fine-grained levels make consolidation-related deformations the dominant issue in this part of the alignment. As we move toward the Belen Viaduct, the soil behavior under dynamic loading conditions becomes critical because of the increasing density of the coarse-grained layers identified as Qal2. In this zone, the predominance of these coarse-grained materials causes liquefaction and dynamic performance of the soil to emerge as the governing geotechnical concerns. The approach fills of the Belen Viaduct reach a height of approximately 14.0 meters, and the groundwater level in this section has been periodically measured and recorded between 3.90 and 9.00 meters during various phases of the project's geotechnical investigations. The groundwater level of 3.90 meters, measured in borehole SK-18+907 during the implementation phase, was considered the most critical condition for design and assessment. Table 5 summarizes the key parameters, including fill height, pre-consolidation and post-stone column settlements, settlements before and after liquefaction, stone column dimensions and spacing, time required for settlement completion.

Table 5. Key Parameters of Settlement and Stone Column Installation

Section	Embankment Height (m)	Maximum Consolidation Settlement (cm)	Settlement Time	Consolidation Settlement Completed Within This Period (cm)	Consolidation Settlement (After Stone Column, cm)	Liquefaction-induced Settlement (cm)	Liquefaction-induced Settlement (After Stone Column, cm)	Stone Column (Spacing-Length, m)
KM: 16+980	9	24	10 months	18.7	5	-	-	S=1.1x1.1 L=16m
KM: 17+145	9	60.1	48 months	55.1	10	-	-	S=1.1x1.1 L=16m
KM: 16+980	14	18.5	6 months	13.5	6	30.99	9.31	S=1.1x1.1 L=20m

Additionally, the geotechnical software Plaxis 2D was used to examine the behavior of embankment constructed on soft ground. The input properties for the soil layers, stone columns, and embankment fill were taken from earlier in-situ research to ensure consistent modeling. The Mohr-Coulomb material model was applied to the embankment fill, soil layers, and stone columns. The stone columns have relatively high unit weights (19 kN/m³ unsaturated and 20 kN/m³ saturated) and a moderate elastic modulus of 8670 kPa, along with high permeability in both horizontal and vertical directions. Stiff clay shows greater stiffness with an elastic modulus of 40000 kPa, but much lower permeability, while soft clay is characterized by lower unit weight, low stiffness (1100 kPa), and very low permeability. The crust layer has intermediate properties, including an elastic modulus of 15000 kPa and slightly higher permeability than the clays. Finally, the road embankment fill has unit weights similar to the stone columns and a stiffness of 15000 kPa, with permeabilities higher than those of the clay layers. Cohesion values range from 1 to 5 kPa, and friction angles vary from 20° in soft clay up to 40° in the stone columns. The expected total consolidation settlement at km: 18+907 is calculated as 18.5 cm before reinforcement (Figure 15a), while after the stone columns with a diameter of 50 cm and a length of 20 m with 1.1 m x 1.1 m spacing, the consolidation settlement is determined as 9.31 cm. Similarly, the liquefaction-induced settlement calculated before and after the stone column is approximately 30.99 and 9.31 cm, respectively as shown in Figure 15b-c.

This study investigates the behavior of highway embankments supported by stone columns under liquefaction-induced settlement. Settlement values were calculated for the clay profiles at critical borehole locations (KM: 16+980, 17+450, and 18+907). The fill materials in these regions are to be placed over alluvial sediments, typically characterized by alternating sequences of plastic and non-plastic gravelly sandy silt and silty sand. At a depth of approximately 20.0 m from the surface, a dense gravelly silty sand/gravel unit continues. In sections where the bridge structures are located, the tolerable settlement amount was taken as 5 cm, and an attempt was made to estimate the time required to wait under the fill load before starting the superstructure construction.

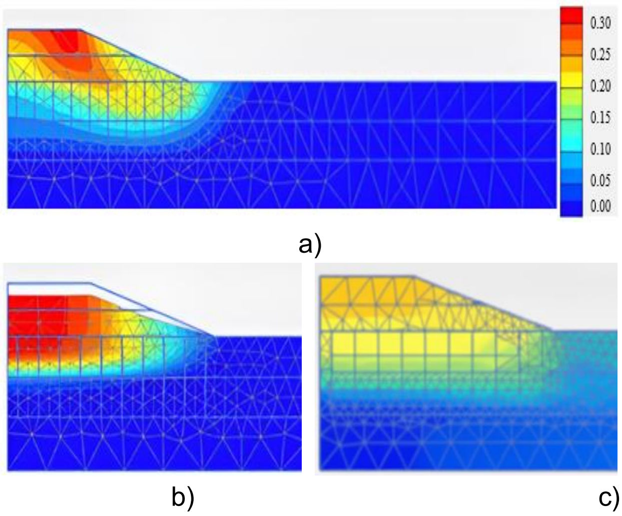

Figure 15. Finite element model: a) Consolidation Settlement, b) Settlement before and c) after Stone column application

5. Conclusions

In section KM:17+145, the amount of clay unit seen in the soil profile and the calculated consolidation settlement amounts in these clay units are well above acceptable limits. It is recommended to make improvements with stone columns in this section. Thus, the total settlement that will occur by increasing the bearing capacity/deformation modulus of the improved soil mass will be reduced. In addition, stone columns will serve as drains, ensuring that the consolidation settlements that will occur in the soil after the construction of the road embankment are completed within a short period of time after construction. In this context, after the improvement with stone columns with a diameter of 50 cm and a length of 16 m with 1.1 m x 1.1 m spacing, the consolidation settlement amount that will occur in the field is determined as 15 cm. It is anticipated that these settlements will be completed within 5-6 months.

Similarly, in section KM:18+907, after the improvement with stone columns with a diameter of 50 cm and a length of 20 m with 1.1 m x 1.1 m spacing, the consolidation settlement in the field is determined as 9 cm. The liquefaction risk under dynamic conditions has been evaluated for the gravelly silty levels observed predominantly in relation to the groundwater level. In this context, there is a need for foundation improvement to minimize the damage that may occur during an earthquake and to ensure usability in emergency situations. Therefore, the application of stone columns was evaluated in order to accelerate settlements in the soil and to increase the relative density of the subsoil specifically, to reduce the excess pore water pressure that will occur under dynamic conditions in the liquefied levels. The findings provide valuable insights into the behavior of stone column-supported structures, allowing engineers and designers to better understand their performance and make informed decisions for future highway embankment projects. Comparing the settlement results from Settle 3D with those from the Plaxis 2D FEM analysis increased confidence in the overall findings, as the two methods produced results that were in good agreement with one another.

Declaration of Ethical Standards

The authors declare that they comply with all ethical standards

Credit Authorship Contribution Statement

Author-1: Conceptualization, investigation, methodology and software, visualization and writing – original draft, review and editing.

Declaration of Competing Interest

The authors have no conflicts of interest to declare regarding the content of this article.

Data Availability Statement

All data generated or analyzed during this study are included in this published article.

6. References

Adalier, K. and Elgamal, A., 2004. Mitigation of liquefaction and associated ground deformations by stone columns. *Engineering Geology*, **72(3–4)**, 275–291. https://doi.org/10.1016/j.enggeo.2003.11.001

Baghel, M. and Memon, K.K., 2023. Soil stabilization using stone columns: a review. *Delta University Scientific Journal,* **6(1),** 39–50. https://doi.org/10.21608/dusj.2023.291006

Baziar, M. and Alizadeh, M., 2015. Evaluation of stone column efficiency for liquefaction mitigation using numerical modeling. *Soils and Foundations*, **55(3)**, 658–670. https://doi.org/10.1016/j.sandf.2015.03.008

Blöcher, G. and Zimmermann, G., 2008. Settle3D – A numerical generator for artificial porous media. *Computers and Geosciences*, **34(12)**, 1827–1842. https://doi.org/10.1016/j.cageo.2007.12.008

Bray, J. D. and Macedo, J. 2017. 6th Ishihara lecture: Simplified procedure for estimating liquefaction-induced building settlement. Soil Dynamics and Earthquake Engineering, **102**, 215-231. https://doi.org/10.1016/j.soildyn.2017.08.026

Cubrinovski, T. and Ishihara, M., 2000. Effects of liquefaction on embankments and countermeasures. *Geotechnique,* **50(3)**, 243–258. https://doi.org/10.1680/geot.2000.50.3.243

Dafalias, Y.F. and Manzari, M.T., 2004. Simple plasticity sand model accounting for fabric change effects. *Journal of Engineering Mechanics*, **130(6)**, pp.622–634. https://doi.org/10.1061/(ASCE)07339399(2004)130:6(622)

Dagli, B.Y., Tuskan, Y. and Gökkuş, Ü., 2018. Evaluation of offshore wind turbine tower dynamics with numerical analysis. *Advances in Civil Engineering*, 2018, Article ID 3054851. https://doi.org/10.1155/2018/3054851

Deb, K., Dash, S.R. and Krishnan, P., 2020. Performance of stone columns in mitigating liquefaction: A critical review. *Soil Dynamics and Earthquake Engineering*, **131,** 106022. https://doi.org/10.1016/j.soildyn.2019.106022

Erdik, M., Zulfikar, C., Sesetyan, K. and Şeşetyan, K., 2006. Türkiye ve yakın çevresinin aktif fayları veri bankası ve deprem tehlikesinin araştırılması. *Yerbilimleri Dergisi*, **34(3),** 1–24.

Girout, R., Blanc, M., Thorel, L. and Dias, D., 2018. Geosynthetic reinforcement of pile-supported embankments. *Geosynthetics International*, **25(1)**, 37–49. https://doi.org/10.1680/jgein.17.00032

Güler, E., Savaş, H. and Afacan, K. B., 2021. Effect of permeability on liquefaction potential of silty sands. Arabian Journal of Geosciences, **14**:1410. https://doi.org/10.1007/s12517-021-07822-9

Hakyemez, H.Y., Göktaş, F. and Erkal, T., 2013. Gediz Grabeninin Kuvaterner Jeolojisi ve Evrimi. *Türkiye Jeoloji Bülteni*, **56(2)**, 1–26.

Hanna, A.M. and Khalifa, M., 2023. Numerical models for shallow foundation on soft clay reinforced with a group of stone columns. *Geomechanics and Geoengineering*, **18(4)**, 309–320. https://doi.org/10.1080/17486025.2022.2046873

Hartono, N. and Fathani, T.F., 2023. Design of stone column to mitigate soil liquefaction: Case study of Yogyakarta International Airport. *Journal of the Civil Engineering Forum*, **9(2),** 195–208. https://doi.org/10.22146/jcef.5933

Ishihara, K., 1996. Soil Behaviour in Earthquake Geotechnics. Oxford University Press.

Jones, K., Pascale, F., Wanigarathna, N., Morga, M. and Sargın, S., 2021. Critical evaluation of the customisation process of the UNDRR disaster resilience scorecard for cities to earthquake-induced soil liquefaction disaster events. *Bulletin of Earthquake Engineering,* **19**, 4115–4143. https://doi.org/10.1007/s10518-020-00993-y

Karayolları Teknik Şartnamesi (KTŞ), 2006.

Koçyiğit, A., Yusufoğlu, H. and Bozkurt, E., 1999. Evidence from the Gediz graben for episodic two-stage extension in western Turkey. *Journal of the Geological Societ*y, **156(3)**, 605–616. https://doi.org/10.1144/gsjgs.156.3.0605

Lai, C. G., Bozzoni, F. and Conca, D. 2021. Technical guidelines for the assessment of earthquake induced liquefaction hazard at urban scale. *Bulletin of Earthquake Engineering,* **19(10),** 4013–4057. https://doi.org/10.1007/s10518-020-00951-8

Liu, H.L., Ng, C.W.W. and Fei, K., 2007. Performance of a geogrid-reinforced and pile-supported highway embankment over soft clay: case study. Journal of *Geotechnical and Geoenvironmental Engineering*, **133(12)**,14831493. https://doi.org/10.1061/(ASCE)10900241(2007)133:12(1483)

Okur, V., 2018. GIS based approach to analyze soil liquefaction and amplification: A case study in Eskisehir, Turkey. *Open Geosciences*, **10(1),** 855–865. https://doi.org/10.1515/geo-2018-0067

Priebe, K., 1997. Design methods for stone columns. *Ground Improvement*, **1(3)**, 127–135. https://doi.org/10.1680/grim.1997.1.3.127

Seed, B. and Idriss, I., 1971. Simplified procedure for evaluating soil liquefaction potential. Journal of the *Soil Mechanics and Foundations Division*, *ASCE*, **97(9)**, 1249–1273. https://doi.org/10.1061/JSFEAQ.000166

Seed, B., Idriss, I. and Arango, R., 1983. Evaluation of liquefaction potential using field performance data. *Journal of Geotechnical Engineering Division, ASCE*, **109(3)**, 458–482. https://doi.org/10.1061/(ASCE)07339410

Selçuk, L. and Kayabali, K., 2015. The design of stone column applications to protect against soil liquefaction. *International Journal of Geotechnical Engineering,* **9(3),** 279–288. https://doi.org/10.1179/1939787914y.0000000063

Singh, A.K. and Mishra, A., 2023. Numerical analysis of embankments on soft clay supported with cement-mixed columns. In: Smart Geotechnics for Smart Societies, CRC Press, 2541–2546.

Stewart, J., 2015. A review of methods for liquefaction evaluation. *Bulletin of the New Zealand Society for Earthquake Engineering,* **48(2)**, 150–160. https://doi.org/10.5459/bnzsee.48.2.150-160

Taube, M.G. and Herridge, J.R., 2002. Stone columns for industrial fills. Nicholson Construction Company, Cuddy, Pennsylvania.

Tokimatsu, Y. and Yoshimi, H., 1990. Empirical correlation of soil liquefaction based on SPT N-value and geotechnical centrifuge tests. *Soils and Foundations*, **30(1),**33–44. https://doi.org/10.3208/sandf1972.30.1_33

Tuskan, Y., 2025. Slope stability evaluation and quantitative landslide risk assessment of road cut-slopes on the D400 highway, southwestern Turkey. *Sādhanā,* **50(4),** 327. https://doi.org/10.1007/s12046-025-02975-9

Tuskan, Y. and Basari, E., 2023. Evaluation of sustainable slope stability with anti-slide piles using an integrated AHP-VIKOR methodology. *Sustainability,* **15(15)**, 12075. https://doi.org/10.3390/su151512075

Tuskan, Y. and Yiğit, M.E., 2025. Investigation of earthquake damage and seismic slope displacements in open irrigation channels using the coupled Eulerian–Lagrangian method. *Quarterly Journal of Engineering Geology and Hydrogeology*, **58(3)**, qjegh2024-162. https://doi.org/10.1144/qjegh2024-162

Van Impe, W. and De Beer, E., 1983. Improvement of settlement behaviour of soft layers by means of stone columns. In: Proc. 8th European Conference on Soil Mechanics and Foundation Engineering, Helsinki, pp.309–312.

Youd, R. and Hoose, T., 1993. Liquefaction resistance of soils from SPT and CPT. In: Proceedings of the H. Bolton Seed Memorial Symposium.

Youd, T.L. and Idriss, I.M., 1997. Proceedings of the NCEER Workshop on Evaluation of Liquefaction Resistance of Soils. Utah, pp.276–276.

Youd, T. L., Idriss, I. M., Andrus, R. D., 2001. Liquefaction Resistance of Soils: Report from the 1996 NCEER and 1998 NCEER/NSF Workshops on Evaluation of Liquefaction Resistance of Soils. Journal of *Geotechnical and Geoenvironmental Engineering, ASCE*, **127(10),** 817–833

Yu, H.-S. and Mitchell, J.K., 1998. Foundation Engineering Handbook. 2nd ed. Springer.

Zhou, Y., Liu, K., Sun, Z.-b. and Chen, Y.-M., 2021. Liquefaction mitigation mechanisms of stone column-improved ground by dynamic centrifuge model tests. *Soil Dynamics and Earthquake Engineering*, **150**, 106946. https://doi.org/10.1016/j.soildyn.2021.106946